☑ 出席國際學術會議心得報告及發表之論文各一份

行政院國家科學委員會專題研究計畫成果報告

旋轉效應對單向固化對流之影響(3/3)

Rotation Effect on Convection in Directional Solidification (3/3)

計劃編號：NSC 89-2212-E-002-124
執行期間：89 年 8 月 1 日至 90 年 7 月 31 日
主持人：陳發林　國立台灣大學應用力學研究所

摘要

本文探討傾斜旋轉對單向固化對流的影響，吾人發現系統此時於流體/固體介面存在一 Ekman 型剪切流。此剪切流扮演穩定或不穩定的角色，則取決於其與平行於介面之旋轉分量的相對角度及大小有關。

關鍵詞：固化，旋轉。

Abstract

In this paper we consider a directionally solidifying alloy under the inclined rotation. There occurs a basic flow induced by the inclination and modified by the rotation. The induced basic flow is of an Ekman spiral form near the melt/solid interface. The direction of the induced flow is steady under the situation of precession-only while periodically changes with time under the spin with/without precession. The effects of the inclined rotation on the stability of the system are investigated by linear analysis. Results show that the onset of the morphological mode is virtually unaffected, while the convective and the mixed modes can be considerably stabilized. The principal stabilizing mechanisms are the rotation vector along the height of the tank and the buoyancy-reduction along the height of the tank. The induced flow may be stabilizing or destabilizing depending on the relative orientation and the amplitude-ratio between the induced flow and the rotation component of the precession along the interface.

Key words: solidification, rotation.

1. Introduction

The directional solidification of a binary alloy, having drawn great research efforts for decades, is the main industrial technique by which many electrical materials of semiconductors such as silicon and gallium-arsenic are produced. During the solidifying process, a melt/solid interface is formed. It is generally need to keep the interface planar in order that the produced materials have the least density of mechanical defects and uniform physical properties.

As the thermal and composition boundary layers form near the interface, a morphological instability (Rutter & Chalmers 1953) may happen and disturb the interface into non-planar shape. The theoretical instability analysis of this problem was first investigated by Mullin

& Sekerka (1964) by using the linear analysis. Another kind of instability can also occur if the rejected solute is lighter or the incorporated solute is heavier than the solvent. Consequently, the density distribution in the compositional boundary layer is hydro-statically unstable. The theoretical analysis of this buoyancy-driven convective instability coupled with the morphological instability was first conducted by Coriell et al. (1980).

In this paper we study a potentially stabilizing method, the inclined rotation, in which the cooling tank is rotated with respect to an axis of inclined angle. Sample and Hellawell (1984) implemented an experiment by this method, in which ammonium chloride solutions were used. They found that the plumes caused by the buoyancy-driven instability in the mush were totally prohibited if the inclined angle reached from 20° to 30°. Chung & Chen (1999) by linear analysis of the mushy layer concluded that the prohibition of the plume is basically due to the buoyancy-reduction along the density gradient when the system is tilted. Because of the large resistance to the flow in the mush, the Coriolis force and the basic flow induced by the inclination are very weak and therefore only have very little to do on stabilizing the mush. In the present situation, the melt, however, should allow a considerably large induced flow and Coriolis effect and consequently a more complicated stability phenomenon. Besides the induced flow, the present system can also contain a rotation vector along the interface due to the precession. Researchers such as Matthew & Cox (1997), Busse & Kropp (1992) and Kropp & Busse (1991) considered the interaction of a shear flow and a horizontal rotating vector in the buoyant convection systems and found that the interaction can be stabilizing or destabilizing in different conditions.

2. Mathematical formulation

Consider a dilute binary alloy of temperature T_∞ and concentration C_∞ solidifying upwards, in which a solid layer is formed below the semi-infinite bulk melt. The melt/solid interface, which is described by $z = h(x, y, t)$, is assumed to be initially planar and advance into the fluid with an average speed V. The cooling tank rotates in such a general way (precession and spin) that the angular velocity can be described by

$$\underline{\dot{\Phi}} = (\dot{\phi}_p \sin\phi_n \sin\phi_s)\underline{e}_x + (\dot{\phi}_p \sin\phi_n \cos\phi_s)\underline{e}_y + (\dot{\phi}_p \cos\phi_n + \dot{\phi}_s)\underline{e}_z ,$$

where ϕ_p, ϕ_n and ϕ_s are the angles of precession, nutation and spin respectively. $\dot{\phi}_p$ and $\dot{\phi}_s$ are the angular velocities of precession and spin respectively. Besides, $\underline{e}_x$, $\underline{e}_y$ and $\underline{e}_z$ are the unit vectors of Cartesian coordinate, which, after taking the Galilean transformation with respect to the interface moving-velocity V, is fixed on the melt/solid interface.

With respect to such a coordinate system, the governing equations in the fluid region $h < z < \infty$ are

$$\nabla \cdot \underline{u} = 0,$$

$$\left[\frac{\partial}{\partial t} - V\frac{\partial}{\partial z} + \underline{u}\cdot\nabla\right]\underline{u} + 2\underline{\dot{\Phi}} \times \underline{u} = -\frac{\nabla P}{\rho_0} + \nu\nabla^2\underline{u} + \left(\frac{\rho}{\rho_0} - 1\right)\underline{g},$$

$$\left(\frac{\partial}{\partial t} - V\frac{\partial}{\partial z} + \underline{u}\cdot\nabla\right)C = D_f\nabla^2 C,$$

$$\left(\frac{\partial}{\partial t} - V\frac{\partial}{\partial z} + \underline{u}\cdot\nabla\right)T = \kappa_f\nabla^2 T.$$

In above equations, $\underline{u}$ is measured with respect to the cooling tank, $P = p - \rho_0 \underline{g}\cdot\underline{r}$, p is the static pressure and ρ_0 is the reference density. Because the rotation speed considered here is less than 5 *rpm*, and the dimension is about 25 *cm* (the horizontal dimension of the cooling tank) we neglect both of the centrifugal force and tangential force in this paper.

In addition, C is the concentration, T the temperature, D_f the solute diffusivity, κ_f the thermal diffusivity of the fluid, ν the kinematic viscosity, and $\underline{g} = -g(\sin\phi_n \sin\phi_s, \sin\phi_n con\phi_s, \cos\phi_n)$ the vector of gravitational acceleration depending on both the nutation and spin angles. Since Boussinesq approximation is applied, the density of the fluid is a constant except in the gravity term where the following relation holds

$$\rho = \rho_0(1 - \alpha(T - T_m) - \beta C),$$

in which α and β are respectively thermal and solute expansion coefficients, and T_m .is the freezing temperature of the pure solvent.

In the solid layer $z < h$, we neglect the diffusion of the solute concentration but consider just the diffusion of the heat, so the heat equation is

$$\left(\frac{\partial}{\partial t} - V\frac{\partial}{\partial z}\right)T = \kappa_s\nabla^2 T,$$

in which κ_s is the thermal diffusivity of the solid phase.

Regarding the boundary condition at infinite far field, we assume that the fluid experiences a rigid-body rotation, and both the concentration and temperature remain the same as the original solution. Accordingly, at $z \to \infty$ we have

$$\underline{u} \to \underline{0},\ C \to C_\infty,\ T \to T_\infty.$$

At the melt/solid interface $z = h(x, y, t)$ the boundary conditions are

$$\underline{u} \times \underline{n} = 0,$$

$$\underline{u} \cdot \underline{n} = 0,$$

$$C_+(1-k)\left(V + \frac{\partial h}{\partial t}\right)\underline{e}_z \cdot \underline{n} = -D_f\frac{\partial C_+}{\partial n},$$

$$T_+ = mC_+ + T_m(1 - \Gamma\varkappa),$$

$$T_+ = T_-,$$

$$L\left(V + \frac{\partial h}{\partial t}\right)\underline{e}_z \cdot \underline{n} = k_s\frac{\partial T_-}{\partial n} - k_f\frac{\partial T_+}{\partial n},$$

where $k = C_-/C_+$ is known as the segregation or partition coefficient, m is the liquidus slope (assumed to be a constant), Γ is the capillary length, $\varkappa$ is the curvature of the interface and L is the latem heat per unit volume of the solid. These boundary conditions respectively express the no-slip condition, the conservation of mass at the interface, the conservation of the solute across the interface, the thermal-dynamical equilibrium condition, the continuity of the temperature across the interface and finally the energy balance at the interface

3. Conclusion

We have considered a binary alloy directionally solidified from below, to which a rotation including spin and/or precession with respect to an inclined axis is imposed. The system admits an analytical basic state including a strong parallel shear flow induced by the inclination and modified by the rotation.

The linear stability analysis shows that the morphological instability is virtually unaffected by the inclined rotation due to the very short characteristic wave-length of the morphological modes. The mix modes and the convective modes, on the other hand, are considerably stabilized. The result for the case of spin and precession indicates that the convective instability can be enhanced if the rotation component along the height of the tank of the precession is opposite in direction to that of the spin. One reason for this is the amplitude-drop of the stabilizing mechanism - the rotation vector along the height of the tank. The other reason is that the interaction between the induced basic flow and the precession component along the interface becomes destabilizing in this situation.

Reference

1. Busse, F. H. & Kropp, M. 1992 Buoyancy driven instabilities in rotating layers with parallel axis of rotation. *ZAMP* 43, 28-35.
2. Chung, C. A. & Chen, F. 1999 Convection in Directionally Solidifying Alloys Under Inclined Rotation. Submitted to *J. Fluid Mech.*
3. Coriell, S. R., Cordes, M. R., Boettinger, W. J. & Sekerka, R. F. 1980 Convective and interfacial instabilities during unidirectional solidification of a binary alloy. *J. Cryst. Growth* **49**, 13-28.
4. Kropp. M. & Busse, F. H. 1991 Thermal convection in differentially rotating system. *Geophys. Astrophys. Fluid Dynamics*. **61**, 127-148.
5. Matthews, P. & Cox, S. 1997 Linear stability of rotating convection in an imposed shear flow. *J. Fluids Mech.* 350, 271-293.
6. Mullins, W. W. & Sekerka, R. F. 1964 Stability of a planar interface during solidification of a binary alloy. *J. Appl. Phys.* **35**, 444-451.
7. Rutter, J. W. & Chalmers, B. A. 1953 A prismatic substructure formed during solidification of metals. *Can J. Phys*. **31**, 15-39.
8. Sample, A. K. & Hellawell, A. 1984 The mechanism of formation and prevention of channel segregation during alloy solidification. *Metall. Trans.* A**15**, 2163-2173.

參加會議報告

報告人：陳發林 教授
台灣大學應用力學所
NSC 89-2212-E-002-124

一、參加會議過程：

此次會議名稱爲「International Conference on Mathematical Model in Continuum Mechanics」，是一種 Workshop 性質的會議。因爲所發表的論文都是大會所邀請，是連體力學各領域具有代表性的題目。此次本人是受德國 Darmstadt 大學 Hutter 教授的邀請參加會議，所發表的論文如附本。此次大會邀請了共八十篇論文，另有十二場大會講席，會議共舉行五天，其中有一天是參觀大學訪問活動。每篇論文以 30 分鐘時間宣讀，且爲避免同時宣讀許多精采論文，故安排的會場不多，所以需四天時間才宣讀完所有論文。

二、參與人員及發表論文

所邀請的論文來自世界各先進國家，如美日歐等西方國家，有些論文也來自東歐及南非。然有四分之一論文是來自德國各大學。本人所發表之論文是有關結晶固化過程中流體變化之連體運動模式及其相關之工業應用。有關此題目之論文並不多，但也在會場中有熱烈的討論。因爲雖然應用有所不同，但理論模式則有雷同之處。除流體力學外，固體力學的論文也占多數，許多新興的研究領域，如生物機電，微觀力學，微機電，生物晶片裡所遇到的力學問題，皆有不少論文發表。

三、與會心得與建議

此次會議給我印象最深的有三項：

（1） 跨領域研究是未來的趨勢：以工學院而言，傳統的土木、機械、電機、化工等分類已不合目前學術發展的趨勢，許多研究題目在工學院裡的訓練已無法完全應付，需跨至醫學院、農學院等，而電機電子類的產品中的許多力學問題更是決定產品品質的關鍵技術，故學術會議應是跨領域者，才能吸引學者參與。

（2） 大會主動邀請論文也是一種趨勢：國際經濟不景氣，學術研究經費大幅刪減，使參加國際會議的學者人數驟降，故除一些傳統的大型國際會議外，許多專業專項會議的規模越來越小。而此次大會的舉辦原則以邀請論文爲主軸，是相當明智的。因爲如此，論文的品質較爲一致，領域較能掌握，講員較有共通性。使與會人士所獲較多。

（3） 我國也可舉辦同類的會議，以主動方式舉辦跨領域國際會議，取代傳統的各工程學會之年會，以增加我國學術的國際曝光率，也使國內學者能同時與許多國際學者齊聚一堂並請教其所專長者。好處甚多。

四、攜回資料：

邀請論文抽印本十多份及大會會議手冊。

Convection in directionally solidifying alloys under inclined rotation

C. A. Chung

Department of Mechanical Engineering, National Central University, Chung-li, Taiwan 320, ROC

Falin Chen

Institute of Applied Mechanics, National Taiwan University, Taipei, Taiwan 10764, ROC

Abstract

We investigate the stability of a dilute binary alloy directionally solidifying upward at a constant rate and spinning around an inclined axis. It is found that prior to the onset of instability, a shear flow is induced by the inclination and modified by the rotation, having the velocity profile like a spiral Ekman-layer flow. Relative to the cooling tank, the induced flow moves periodically at a frequency equal to that of the spin. Based on this basic-state flow, the effects of the inclined spin on both the morphological and convective instabilities of the system are examined by linear analysis. Results show that the morphological modes caused by the constitutional supercooling acting on the melt-solid interface are somewhat stabilized; the convective modes arising from the compositional buoyancy developing above the interface can be considerably suppressed. The effective stabilizing factors include the basic-state flow, the Coriolis force due to spin and the reduction of buoyancy along the height of the tank due to inclination.

1. Introduction

During the directional solidification of a binary alloy, the interface may become unstable to a cellular structure, ultimately leading to unwanted compositional inhomogeneity in the final casting. This is referred to as morphological instability (Rutter & Chalmers 1953), a long trouble issue in the microchip manufacturing technology. The perturbed interface encounters the supercooled melt and starts to grow, rendering the interface unstable (Mullin & Sekerka 1964). The interface can also lose its planar shape due to convective instability. This convective motion of fluid may occur once there forms an unstable density distribution in the residual liquid above the interface. Coriell et al. (1980) investigated this buoyancy-driven instability coupled with the morphological instability. They showed that the convective instability is characterized by a wavelength comparable to the thickness of the compositional boundary layer while the wavelength of the morphological mode is much shorter.

To refrain the castings from the compositional inhomogeneity, investigating the effects of a shear flow on the solidification of alloys has been discussed widely (Glickman et al. 1986, Brattkus and Davis 1988, Forth and Wheeler 1992, Davis and Schulze 1996). Mostly, these investigations drew two general conclusions. First, because the morphological instability is characterized by its quite small wavelength, it can hardly feel the shear flows. Therefore, the morphological mode is only slightly stabilized. Second, the imposed shear flows influence both the morphological and convective instabilities by selecting favored oriented rolls. Another potential means to prevent castings from becoming inhomogeneous in composition is to apply rotation. Oztekin & Pearlstein (1992) showed that a vertical rotation in general stabilizes the convective mode. However as the direction of the flow induced by the morphological instability is virtually normal to the melt-solid interface due to the small wavelength, no Coriolis force by the induced flow can be generated to inhibit the instability. The vertical rotation has only weak effects on the morphological mode.

In this paper, we propose an alternative scheme – inclined spin, which is supposed to contain both the stabilization effects of shear flow and rotation. This scheme is motivated by the experiment of Sample and Hellawell (1984) and the analytical analysis of Chung and Chen (2000). They showed that by this means the formation of chimneys in the mushy zone of a solidifying alloy can be largely suppressed. Besides, with the inclination there is a shear flow induced neutrally by the gravity and modified by the rotation. Unlike previous studies in which most of the shear flows were artificially imposed, this scheme therefore is more feasible for industrial purpose.

2. Problem description and formulation

We consider a dilute binary alloy of initial temperature T_∞ and concentration C_∞, which is solidified from below so that a solid region forms below the semi-infinite bulk melt. The melt-solid interface described by $z = h(x, y, t)$ is assumed initially planar and advancing into the bulk melt at a constant speed V. The cooling tank spins around an inclined axis that the angular velocity can be described as $\dot{\Phi} = \dot{\phi}_s \boldsymbol{e}_z$. Here $\dot{\phi}_s$ is the angular velocity of spin and $\boldsymbol{e}_z$ is the unit vector in the z-direction of the reference coordinate fixed on the melt-solid interface, rotating with the cooling tank and translating upward at the velocity V. The governing equations in the fluid region $h < z < \infty$ include the conservation of mass, momentum, solute and heat. Since the Boussinesq approximation is applied, the density of the fluid is assumed constant except in the gravity term where the relation holds $\rho = \rho_0 (1 - \alpha(T - T_m) - \beta C)$. Here α and β are respectively the thermal and solute expansion coefficients and T_m is the freezing temperature of the corresponding pure solvent. In the solid region $z < h$, we neglect the diffusion of solute while consider the heat balance only. The governing equations are made dimensionless with the solute-field scale. Namely, V is for velocity, $H = D/V$ for length (D the solute diffusivity), D/V^2 for time, C_∞ for concentration, T_m for temperature, and $\nu \rho_0 V^2 / D$ for pressure (ν the kinematic viscosity). To nondimensionalize the temperature, we subtract T_m from the dimensional temperature before dividing it with the scale. The dimensionless governing equations in the fluid region are

$$\nabla \cdot \boldsymbol{u} = 0, \tag{1a}$$

$$\frac{1}{S_c}\left(\frac{\partial}{\partial t} - \frac{\partial}{\partial z} + \boldsymbol{u} \cdot \nabla\right)\boldsymbol{u} = \nabla^2 \boldsymbol{u} - \nabla p + (R_c C + R_t T)[S_n S_s(t) \boldsymbol{e}_x + S_n C_s(t) \boldsymbol{e}_y + C_n \boldsymbol{e}_z] + T_a^{1/2} \boldsymbol{u} \times \boldsymbol{e}_z, \tag{1b}$$

$$\left(\frac{\partial}{\partial t} - \frac{\partial}{\partial z} + \boldsymbol{u} \cdot \nabla\right) C = \nabla^2 C, \tag{1c}$$

$$\frac{1}{L_e}\left(\frac{\partial}{\partial t} - \frac{\partial}{\partial z} + \boldsymbol{u} \cdot \nabla\right) T = \nabla^2 T. \tag{1d}$$

The dimensionless heat equation in the solid region is

$$\frac{1}{L_s}\left(\frac{\partial}{\partial t} - \frac{\partial}{\partial z}\right) T = \nabla^2 T. \tag{2}$$

In these equations, $S_c \equiv \nu / D$ is the Schmidt number, $L_e \equiv \kappa_f / D$ the Lewis number of the fluid (κ_f the thermal diffusivity of the fluid), $L_s \equiv \kappa_s / D$ the Lewis number of the solid (κ_s the thermal diffusivity of the solid). R_c and R_t are respectively the solutal and thermal Rayleigh numbers defined as $R_c \equiv g \beta C_\infty H^3 / \nu D$, $R_t \equiv g \alpha T_m H^3 / \nu D$, where g is the gravitational constant. Furthermore, in equation (1b) T_a is the Taylor number of spin accounting for the intensity of spin, defined as $T_a \equiv (2H^2 \dot{\phi}_s / \nu)^2$. For simplification, we have adopted the abbreviations $S_n \equiv \sin \phi_n$, $C_n \equiv \cos \phi_n$, $S_s(t) \equiv \sin(\Omega t)$ and $C_s(t) \equiv \cos(\Omega t)$, where ϕ_n is the tilt angle and Ω is the dimensionless angular velocity of spin, which is related with T_a by the relation $\Omega \equiv S_c T_a^{1/2} / 2$. Note that in the momentum equation, we have neglected the centrifugal force and considered the Coriolis effect of spin only.

Regarding the boundary conditions, we assume that the fluid in the far field experiences a rigid-body rotation and both the concentration and temperature remain their original values. Namely, the height of the tank is assumed large enough so that the influence of the possible deformation of the free surface on the fluid motion near the melt-solid interface is ignored. Accordingly, at $z\to\infty$ the dimensionless boundary conditions are

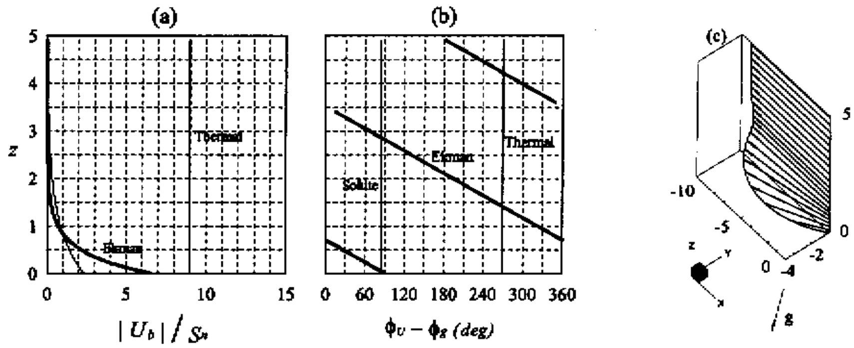

Figure 1. The distribution of the basic-state velocity along the height of the cooling tank for $T_e = 10$: the solute-layer flow, thermal-layer flow and Ekman-layer flow. (a) The amplitude. (b) The phase angle measured from the gravity component in the (x, y)-plane. (c) The overall velocity vector of the basic-state velocity.

$$\boldsymbol{u}\to 0,\quad C\to 1,\quad T\to T_\infty . \tag{3a-c}$$

At the melt-solid interface $z=h(x,y,t)$, the dimensionless boundary conditions are

$$\boldsymbol{u}\times\boldsymbol{n}=0,\quad \boldsymbol{u}\cdot\boldsymbol{n}=0,\quad (k-1)C_+\left(1+\frac{\partial h}{\partial t}\right)\boldsymbol{e}_z\cdot\boldsymbol{n}=\nabla C_+\cdot\boldsymbol{n},\quad T_+=MC_+-\mathsf{U}\mathsf{K}, \tag{4 a-d}$$

$$T_-=T_+,\quad \mathsf{L}\left(1+\frac{\partial h}{\partial t}\right)\boldsymbol{e}_z\cdot\boldsymbol{n}=\left(L_s\nabla T_- - L_e\nabla T_+\right)\cdot\boldsymbol{n}. \tag{4e, f}$$

In these equations $\boldsymbol{n}$ is the normal vector to the interface directing toward the melt. Subscripts + and - denote respectively the quantities right above and below the interface, $k=C_-/C_+$ is the segregation or partition coefficient, $M\equiv mC_\infty/T_m$ is the dimensionless liquidus slope (m is the dimensional liquidus slope assumed to be a constant). Meanwhile, we have included the capillary effect (the Gibbs-Thompson effect) in equation (4d), where $\mathsf{U}\equiv\Gamma V/D$ means the dimensionless capillary length, Γ the dimensional capillary length and K the curvature of the interface (assumed negative for a concave projection into the fluid). Finally, $\mathsf{L}\equiv L/T_m(\rho c_p)_-$ is the Stefan number and L is the latern heat per unit volume of the solid. It is noted that in equation (4f), we have neglected the difference of the specific heat between the solid and liquid phases. For detailed physical meanings of these interface conditions, readers can reference Forth and Wheeler (1992).

3. Basic-state solution

We assume a much larger horizontal dimension of the cooling tank than the characteristic length scale. By means of scaling analysis, the continuity equation yields that the velocity component in the z-direction is much weaker than that in the (x, y)-plane. The velocity in the z-direction is thus negligible for the basic state. We also assume the space-differentiation to both the x- and y-coordinate are negligible compared with that to the z-coordinate. Consequently, the basic state is independent of x and y. The basic flow is induced by the gravity component in the (x, y)-plane owing to the inclination. As the induced flow is parallel with the (x, y)-plane, the basic-state temperature and concentration are not affected by it. Therefore, they are similar to those shown in previous studies such as Forth & Wheeler (1992). Because the fluid in the far field is assumed to rotate with the cooling tank like a rigid body, the consideration of equations (1b) gives the following form of the basic-state pressure

$$p_b=\bar{p}_b(z,t)+\left(R_c+R_tT_\infty\right)\left[xS_nS_s(t)+yS_nC_s(t)+zC_n\right], \tag{5}$$

where the reduced pressure $\bar{p}_b$ can be solved by substituting equation (5) into equation (1b). The basic-state pressure can no longer balance the fluid weight in the (x, y)-plane since the fluid density is not constant along the height of the tank. This unbalance between the pressure and the fluid weight consequently induces the basic flow, which is then modified by the Coriolis force of spin. The velocity components in the x-and y-direction are

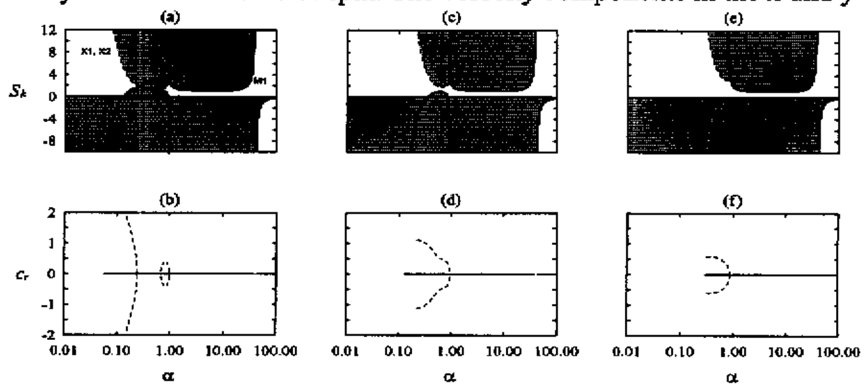

Figure 2. The neutral curves in terms of the Sekerka number S_k, the wave speed c_r and the wave number α for the case of vertical rotation where the tilt angle $\phi_n = 0$. The gray areas indicate unstable regions. The labels UM, M1, M2, C1, C2, X1 and X2 denote the different instability modes. (a)(b) $T_a = 0$, (c)(d) $T_a = 1$, (e)(f) $T_a = 4$.

obtained by substituting equation (5) into equations (1b), giving

$$U_b \equiv u_b + iv_b = \hat{U}_b(z)e^{i\phi_g}, \tag{6}$$

In this complex expression, $\hat{U}_b$, a function of z only, is the velocity amplitude having the following form

$$\hat{U}_b(z) = -\frac{S_n R_c G_c}{\Delta_c}\exp(i\phi_c - z) - \frac{S_n R_t L_e G_t}{\Delta_t}\exp(i\phi_t - z/L_e) + \left[\frac{S_n R_c G_c}{\Delta_c}e^{i\phi_c} + \frac{S_n R_t L_e G_t}{\Delta_t}e^{i\phi_t}\right]\exp(-ibz - z/d_E). \tag{7}$$

Here $\phi_g = -(\Omega t + \pi/2)$ is defined as the phase angle of the gravity vector with respect to the cooling tank. The remaining parameters in equation (7) are defined as follows.

$$d_E = 1\Big/\left(\frac{1}{2S_c} + a\right),\quad a = \left[\left(\frac{1}{S_c^2} + \sqrt{\frac{1}{S_c^4} + 16T_e^2}\right)\Big/8\right]^{1/2},\quad b = \frac{T_e}{|T_e|}\left[\left(-\frac{1}{S_c^2} + \sqrt{\frac{1}{S_c^4} + 16T_e^2}\right)\Big/8\right]^{1/2}, \tag{8a-c}$$

$$\Delta_c = \left((1 - 1/S_c)^2 + T_e^2\right)^{1/2},\quad \cos\phi_c = \frac{1 - 1/S_c}{\Delta_c},\quad \sin\phi_c = \frac{T_e}{\Delta_c}, \tag{8d-f}$$

$$\Delta_t = \left(((1/L_e - 1/S_c)/L_e)^2 + T_e^2\right)^{1/2},\quad \cos\phi_t = \frac{(1/L_e - 1/S_c)/L_e}{\Delta_t},\quad \sin\phi_t = \frac{T_e}{\Delta_t}. \tag{8g-i}$$

Further, in equation (7) the local gradients of the concentration and temperature are defined respectively as $G_c = (k-1)/k$, $G_t = (T_\infty - M/k)/L_e$, and in equation (8) $T_e \equiv T_a^{1/2}/2$ is an effective Taylor number used to simplify the writing. Equation (7) indicates that the induced velocity increases in amplitude with inclined angle and changes its direction periodically with time at a frequency equal to the spin angular velocity Ω. Furthermore, the induced velocity changes with height, consisting of three different parts according to the length scale: the solute-layer flow, the thermal-layer flow and the Ekman-layer flow. To illustrate these three parts, we display in figure 1 their distributions with height for $T_a = 10$. For all the computations in this paper, we have used the parameter values S_c =81, L_e =3600, L_s =6700, R_c =10, R_t =250, k =0.3, $G_l = 10^{-4}$, L =0.29. These values are corresponding to the model lead-tin alloy considered by Coriell et al. (1980). In figure 1a, one can see the velocities of both the solute-layer flow and the Ekman-layer flow decrease exponentially with height. The velocity of the thermal-layer flow seems to remain virtually constant in magnitude near the solid-melt interface because the Lewis number has been considered large, leading to a deep thermal boundary layer for this case. It is evident from figure 1b that both the solute-layer flow and thermal-layer flow do not change their directions, whereas the Ekman-layer flow varies in direction periodically with height by a period $2\pi/b$. Please note that in figure 1b we have adopted ϕ_g, the orientation of the gravity component in the (x, y)-plane, as the reference angle to measure the flow direction. In figure 1c, we show the velocity vector of the induced flow. The overall induced

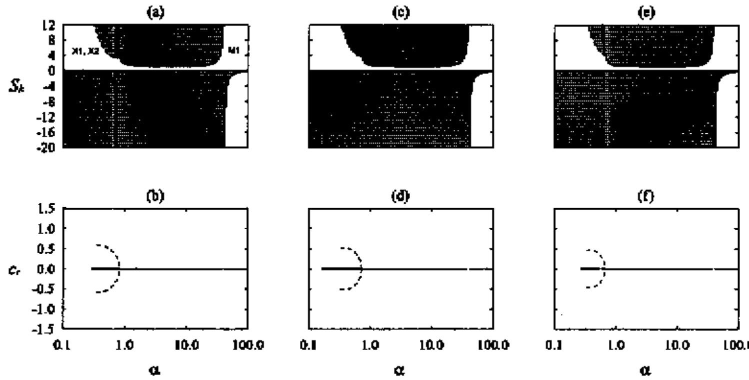

Figure 3. The neutral curves in terms of the Sekerka number S_k, the wave speed c_r and the wave number α for the case of inclined spin. The velocity of spin is set to $\Omega = 80$. The tilt angle ϕ_n has different values: (a)(b) $\phi_n = 10°$, (c)(d) $\phi_n = 20°$, (e)(f) $\phi_n = 25°$.

flow in the far field stays in the (x, z)-plane, while near the interface it has a component in the y-direction.

4. Linear stability analysis

We investigate the stability feature of the basic state, focusing on the effects of the inclined spin. To simplify the analysis, the frozen temperature assumption (Forth & Wheeler 1989, 1992) has been employed, i. e., the temperature is fixed at its basic-state value. Except temperature, we introduce small perturbations together with the basic state into the governing equations (1) and then neglect the products of the small quantities to obtain the linear perturbation equations. These perturbation equations and boundary conditions are nonetheless too tedious to be presented in the text. However, two new dimensionless parameters need to be addressed: the modified capillary parameter $U^* = U/MG_c$ and the Sekerka number $S_k = MG_c/G_l$ that measures the intensity of the super-cooling effect at the interface. For the following computations, we choose $U^* = 6.131\times10^{-4}$. The basic flow is a periodical function of time varying with a frequency equal to the spin angular velocity Ω. Therefore, the perturbation equations contain time-dependent coefficients and need to be solved by employing the Floquet theory (Chung and Chen 2000), expanding the time-dependent variable by a complex Fourier series of time.

To reveal the effects of the inclined spin, we first demonstrate for comparison the result of a stationary-cooling tank. Figure 2a shows the neutral curves of the morphological modes M1, M2 and UM (thin curves), the convective modes C1 and C2 (thick curves) and the mixed modes X1 and X2 (dotted curves). Figure 2b displays their wave speeds $c_r = -\omega_i/\alpha$ of the instability modes. In these figures, we have adopted the same labels used by Forth and Wheeler (1992) to name the instability modes. The shadow areas denote the unstable regions of the instabilities. As shown, the solution exhibits a so-called folding structure for the mixed modes X1 and X2, which have the same onset condition while travel in the opposite directions. The X1 moves with forward wave speed $+c_r$ and the X2 backward wave speed $-c_r$. The stationary C1 and M1 modes are connected by the X1, X2 modes, generating two other stationary modes C2 and M2. Note that the UM mode is also stationary but physically unrealistic because it occurs with non-positive Sekerka number.

Two sets of figure are displayed for $T_a = 1$ (figure 2c, d, equivalent to 0.5 rpm corresponding to the lead-tin alloy considered) and $T_a = 4$ (figure 2e, f, equivalent to 1 rpm) to demonstrate the influences of vertical rotation. It is discovered that, once the vertical rotation is applied, the coalescence between the C1, X1 and X2 modes becomes disconnected and the mode M2 disappears. The convective mode C1 and mixed modes X1, X2 are suppressed by the vertical rotation through the action of the Coriolis force, as commonly found in previous studies (Oztekin and Pearlstein 1991). The morphological mode M1, however, is virtually unaffected primarily due to the short wavelength (Forth and Wheeler 1992).

To show the influence of inclined spin, we show in figure 3 the neutral curves for the case of $\Omega = 80$ (equivalent to $T_a = 4$ and 1 rpm for present system) with the tilt angle ϕ_n varying from $10°$ to $25°$. We see in figure 3a the mixed modes X1, X2 and the convective modes C1, C2 are largely stabilized due to the actions of the induced flow and the gravity shifted by the inclination. As the tilt angle increases (Figures 3c and 3e), the stabilization is more enhanced. The morphological mode M1, on the other hand, is only slightly stabilized owing to it short characteristic wavelength. Note that the instability modes C1, C2, M1 and UM having $c_r = 0$ are moving synchronously with the spin. Whereas the instability modes X1 and X2 have $c_r \neq 0$, indicating that the mixed modes are non-synchronous. Their frequencies are modulated by $\omega_i = -\alpha c_r$.

5. Conclusions

We have analyzed the stability characteristics of a binary alloy that is directionally solidified upward and spinning around an inclined axis. The system has a basic state, in which a strong helical shear flow is induced naturally by the inclination and modified by the rotation, not like previous studies where the shear flow is often artificially imposed. Changing in direction periodically by a frequency equal to spin, increasing in amplitude with the inclined angle and decreasing with increasing spin speed, the induced flow comprises three parts. They are the solute-layer flow, the thermal-layer flow and the spiral Ekman-layer flow. Stability analysis shows that once the inclined spin is imposed, the convective modes and morphological modes, which are of stationary onset with a vertical cooling tank, occur synchronously with the spin motion. The mixed modes, in contrast, which are originally of oscillatory onset, occur non-synchronously with the spin. In the context of the stability condition, the mixed mode and convective mode are largely stabilized by the inclined spin. The morphological instability, on the other hand, is somewhat stabilized.

Acknowledgments

The authors greatly appreciate the fund from the National Science Council of Taiwan through Grant No. NSC 88-2212-E-002-018.

References

K. Brattkus and S. H. Davis, Flow induced morphological instabilities: Stagnation-point flows, J. Cryst. Growth, vol. 89, pp. 423-427, 1988.

C. A. Chung, and F. Chen, Convection in Directionally solidifying alloys under inclined rotation, J. Fluid Mech., vol. 412, pp. 93-123, 2000.

S. R. Coriell, M. R. Cordes, W. J. Boettinger and R. F. Sekerka, Convective and interfacial instabilities during unidirectional solidification of a binary alloy, J. Cryst. Growth, vol. 49, pp. 13-28, 1980.

S. H. Davis and T. P. Schulze, Effects of flow on morphological stability during directional solidification, Metall. Mater. Trans., vol. 27A, pp. 583-594, 1996.

S. A. Forth and A. A. Wheeler, Coupled convective and morphological instability in a simple model of the solidification of a binary alloy, including a shear flow, J. Fluid Mech., vol. 236, pp. 61-94, 1992.

M. E. Glickman, S. R. Coriell and G. B. McFadden, Interaction of flows with the crystal-melt interface, Ann. Rev. Fluid Mech., vol. 18, pp. 307-335, 1986.

W. W. Mullins, R. F. Sekerka, Stability of a planar interface during solidification of a binary alloy, J. Appl. Phys, vol. 35, pp. 444-451, 1964.

A. Oztekin, and A. J. Pearlstein, Coriolis effects on the stability of plane-front solidification of dilute Pb-Sn binary alloys, Metall Trans. Vol. 23b, pp. 73-80, 1991.

J. W. Rutter and B. A. Chalmers, A prismatic substructure formed during solidification of metals, Can J. Phys., vol. 31, pp. 15-39, 1953.

A. K. Sample and A. Hellawell, The mechanism of formation and prevention of channel segregation during alloy solidification, Metall. Trans., vol. A15, pp. 2163-2173, 1984.